

Molecular Dynamics Simulation Study on Two-Component Solubility Parameters of Carbon Nanotubes and Precisely Tailoring the Thermodynamic Compatibility between Carbon Nanotubes and Polymers

Yanlong Luo,* Xianling Chen, Sizhu Wu, Songyuan Cao, Zhenyang Luo,* and Yijun Shi



Cite This: *Langmuir* 2020, 36, 9291–9305



Read Online

ACCESS |



Metrics & More

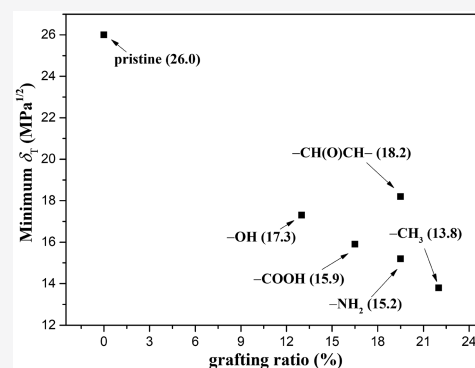


Article Recommendations



Supporting Information

ABSTRACT: Solubility parameters play an important role in predicting compatibility between components. The current study on solubility parameters of carbon materials (graphene, carbon nanotubes, and fullerene, etc.) is unsatisfactory and stagnant due to experimental limitations, especially the lack of a quantitative relationship between functional groups and solubility parameters. Fundamental understanding of the high-performance nanocomposites obtained by carbon material modification is scarce. Therefore, in the past, the trial and error method was often used for the modification of carbon materials, and no theory has been formed to guide the experiment. In this work, the effect of defects, size, and the number of walls on the Hildebrand solubility parameter (δ_T) of carbon nanotubes (CNTs) was investigated by molecular dynamics (MD) simulation. Besides, three-component Hansen solubility parameters (δ_D , δ_p , δ_H) were transformed into two-component solubility parameters (δ_{vdW} , δ_{elec}). The quantitative relation between functional groups and two-component solubility parameters of single-walled carbon nanotubes (SWCNTs) was then given. An important finding is that the δ_T and δ_{vdW} of SWCNTs first decrease, reach a minimum, and then increase with increasing grafting ratio. The thermodynamic compatibility between functionalized SWCNTs and six typical polymers was investigated by the Flory–Huggins mixing model. Two-component solubility parameters were proven to be able to effectively predict their compatibility. Importantly, we theoretically gave the optimum grafting ratio at which the compatibility between functionalized SWCNTs and polymers is the best. The functionalization principle of SWCNTs toward good compatibility between SWCNTs and polymers was also given. This study gives a new insight into the solubility parameters of functionalized SWCNTs and provides theoretical guidance for the preparation of high-performance SWCNTs/polymers composites.



INTRODUCTION

Carbon nanotubes (CNTs) have been widely used in polymer composites, sensing, catalytic and energy fields due to its intriguing and excellent mechanical, thermal, electrical, optical and chemical properties.^{1–4} In the field of polymer nanocomposites (PNCs), a small amount of CNTs can endow polymers excellent dielectric, thermal, electromagnetic shielding, and other functional properties due to the large aspect ratio and high specific surface area of CNTs.^{5–7} It is generally known that CNT–polymer interactions and CNT dispersion are two principal factors determining the resulting properties of the composites. From the view of thermodynamics, the compatibility between the matrix and filler plays a crucial role in matrix–filler interactions and filler dispersion. Therefore, the compatibility is one of the focuses in the field of PNCs. Previous studies indicated that the pristine CNTs without any defects have poor compatibility with the polymeric matrix so that only the functionalization of CNTs can obtain

high-performance CNTs/polymers composites.^{8–10} For example, the introduction of oxygen-containing groups into the surface of CNTs by strong oxidation treatment has been proven to be an effective method for improving the compatibility between CNTs and polymers.⁸ Meanwhile, the introduction of defects is ineluctable in the process of strong oxidation treatment, which will cause significant changes in the physical and chemical properties of CNTs.^{11,12}

The common way to predict the compatibility between two components is to compare their solubility parameters.^{13,14} The two most commonly used solubility parameters were proposed

Received: June 12, 2020

Revised: July 27, 2020

Published: July 27, 2020



by Hildebrand and Hansen.^{15,16} The Hildebrand solubility parameter (δ_T) is the square root of cohesive energy density (CED), and the CED is simply the cohesive energy (E_{coh}) per unit of volume (V):¹⁷

$$\delta_T = \sqrt{\text{CED}} = \sqrt{\frac{E_{\text{coh}}}{V}} \quad (1)$$

The intermolecular interactions are composed of dispersive ($E_{\text{coh,D}}$), polar ($E_{\text{coh,P}}$), and hydrogen bonding ($E_{\text{coh,H}}$) interactions, so the Hansen solubility parameters (δ_i , $i = \text{D, P, H}$) were proposed as follows:¹⁸

$$\delta_D = \sqrt{\frac{E_{\text{coh,D}}}{V}}, \quad \delta_P = \sqrt{\frac{E_{\text{coh,P}}}{V}}, \quad \delta_H = \sqrt{\frac{E_{\text{coh,H}}}{V}} \quad (2)$$

Then the relation between Hansen and Hildebrand solubility parameters as follows:

$$\delta_T^2 = \delta_D^2 + \delta_P^2 + \delta_H^2 \quad (3)$$

Generally, the Hildebrand solubility parameter can predict the compatibility of nonpolar polymer and nonpolar solvent well, while Hansen solubility parameters are considered to be more effective in predicting the compatibility of polar polymers.¹⁸ In the past, most studies focused on the solubility parameters of polymers and small molecules, as well as their compatibility.^{19–21} In recent years, many studies have reported Hildebrand and Hansen solubility parameters of some carbon materials (graphene,²² CNTs,^{23–26} fullerene,²⁷ and carbon fiber,²⁸ etc.). Additionally, great progress has been made in the compatibility and their properties prediction of PNCs filled with carbon materials based on solubility parameters.^{23,27,29} For example, Bergin et al.²⁴ found that the Hildebrand solubility parameter of high-pressure CO conversion single-walled carbon nanotubes (HiPCO-SWCNTs) is $\delta_T = 20.8 \text{ MPa}^{1/2}$ and the Hansen solubility parameters are $\delta_D = 17.8 \text{ MPa}^{1/2}$, $\delta_P = 7.5 \text{ MPa}^{1/2}$, and $\delta_H = 7.6 \text{ MPa}^{1/2}$. Ata et al.²³ found that the matching solubility parameters between CNTs and rubbers are important to obtain higher electrical conductivity of CNTs/rubbers composites. It was also found that the matching solubility parameters are crucial to achieve a higher mechanical property and lower percolation threshold of CNTs/polysulfone composites.²⁹ To the best of our knowledge, most current studies focus on the solubility parameters of pristine CNTs as well as the compatibility between pristine CNTs and polymers. Although a few experiments have attempted to measure the solubility parameters of functionalized CNTs,^{30,31} the quantitative relation between functional groups and solubility parameters of CNTs is still lacking so that there is no theoretical guidance for the functionalization of CNTs for high-performance CNTs/composites. This may be because it is difficult to realize the quantitative control and characterization of functional groups on the surface of CNTs by current experimental means. Besides, a large number of solvents are needed to measure the solubility parameters by the experimental method, which not only takes a lot of time but also causes environmental pollution.

Alternatively, molecular dynamics (MD) simulation based on force field methods has been proven to be a powerful technique for predicting the relationship between the structure and properties of materials.^{32–34} Especially with the development of accurate ab initio force fields, MD simulation has been successfully employed to give a molecular-level insight into the microstructure, thermodynamic, thermal conductivity, and

mechanical properties of polymers (e.g., polyethylene,³⁵ epoxy,³⁶ natural rubber,³⁷ polyamide,³⁸ poly(methyl methacrylate),³⁶ and polyacrylonitrile³⁹) composites filled with CNTs. At present, the solubility parameters of many small molecules and polymers, as well as their compatibility, have been studied through MD simulation.^{16,40} Gupta et al.⁴⁰ calculated the electrostatic and van der Waals components of solubility parameters of indomethacin drug and polymeric carriers through MD simulation and effectively predicted the miscibility of pharmaceutical compounds. Although a small amount of literature has reported the solubility parameters of CNTs by MD simulation,^{34,41} it mainly focuses on that of the pristine CNTs, and the solubility parameters of functionalized CNTs have not been reported. Maiti et al.⁴¹ first employed different force fields to calculate the δ_T of pristine SWCNTs as a function of tube diameter and explored the CNTs dispersion in the polymer matrix from a Flory–Huggins theory point of view. On the basis of Maiti's work, Lee et al.³⁴ reported the electrostatic and van der Waals components of solubility parameters of pristine SWCNTs and pristine double-walled carbon nanotubes (DWCNTs) as a function of tube length and diameter by using a finite-length model. The unique advantages of MD simulation in quantification can make up for the disadvantage of the experimental method for studying the solubility parameters of functionalized CNTs to a certain extent. Therefore, MD simulation can be expected to give the quantitative relation between functional groups and solubility parameters of CNTs and be an effective method for exploring the compatibility between functionalized CNTs and polymers.

In this work, the effect of defects, size, the number of walls and functional groups including hydroxyl ($-\text{OH}$), amino ($-\text{NH}_2$), methyl ($-\text{CH}_3$), carboxyl ($-\text{COOH}$), and epoxy ($-\text{CH}(\text{O})\text{CH}-$) groups on solubility parameters of CNTs was explored. Three-component Hansen solubility parameters were transformed into two-component solubility parameters. Six typical polymers including polyethylene (PE), polystyrene (PS), polyvinyl chloride (PVC), natural rubber (NR), nitrile butadiene rubber (NBR), and bisphenol A epoxy resin (EP) were selected to investigate whether two-component solubility parameters can predict effectively the compatibility between functionalized SWCNTs and polymers. Additionally, the optimum grafting ratio for the best compatibility between functionalized SWCNTs and polymers was investigated. At last, the functionalization principle of SWCNTs toward good compatibility was explored.

METHODOLOGY

Transformation of Hansen Solubility Parameters. At present, the most common force field for all-atom MD simulation of polymer and carbon materials systems is an ab initio Condensed-phase Optimized Molecular Potentials for Atomistic Simulation Studies (COMPASS) force field due to its accurate and simultaneous prediction of condensed-phase properties.^{42,43} The potential energy (E_{total}) of a system can be expressed as a sum of valence (E_{valence}), crossterm ($E_{\text{crossterm}}$), and nonbond (E_{nonbond}) interactions in COMAPSS force field:

$$E_{\text{total}} = E_{\text{valence}} + E_{\text{crossterm}} + E_{\text{nonbond}} \quad (4)$$

The E_{valence} is the sum of bond stretching, valence angle bending, dihedral angle torsion, out-of-plane interactions, and the $E_{\text{crossterm}}$ is included to achieve higher accuracy by accounting for such factors as bond or angle distortions

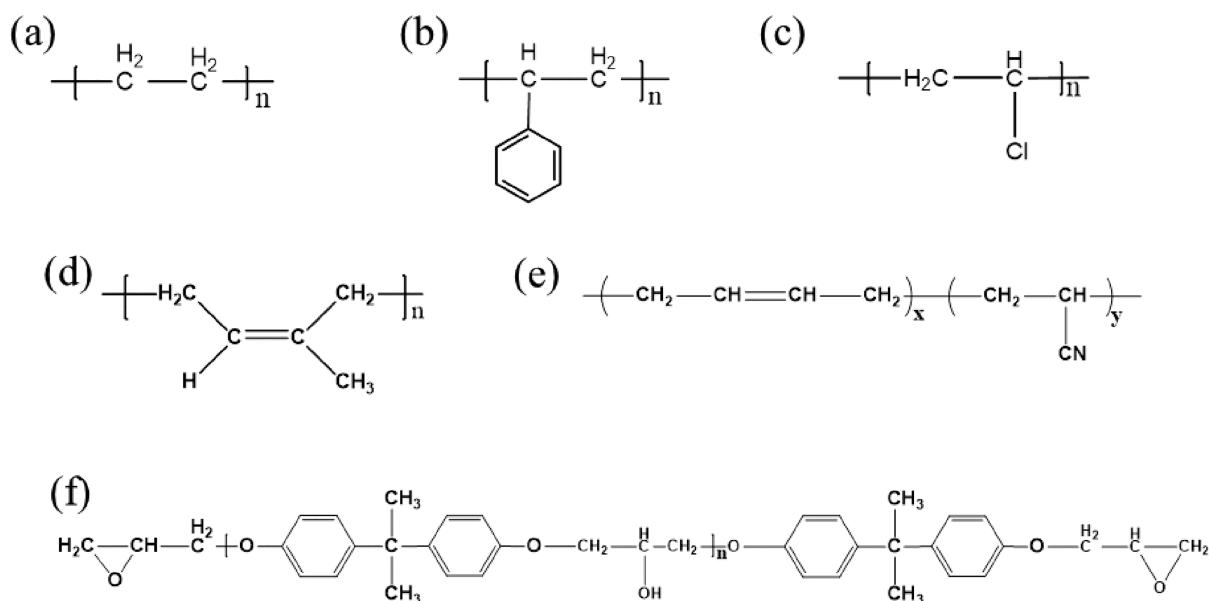


Figure 1. Chemical formulas of (a) PE, (b) PS, (c) PVC, (d) NR, (e) NBR, and (f) EP. In the simulation, the degree of polymerization, n , is 50. The mass fraction of acrylonitrile and butadiene in NBR is 41% and 59%, respectively.

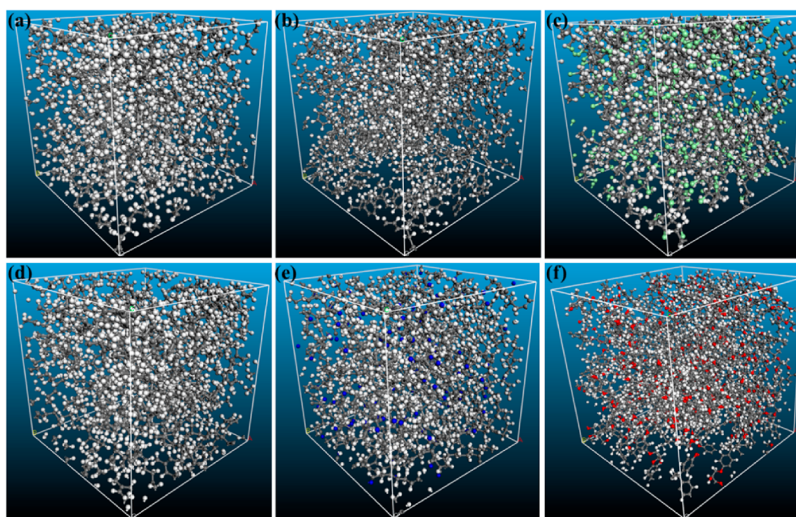


Figure 2. Amorphous cells of (a) PE, (b) PS, (c) PVC, (d) NR, (e) NBR, and (f) EP (gray, white, red, blue, and green balls represent C, H, O, N, and Cl atoms, respectively).

caused by nearby atoms. The E_{nonbond} is the sum of van der Waals (E_{vdW}) and electrostatic (E_{elec}) interactions:

$$E_{\text{nonbond}} = E_{\text{vdW}} + E_{\text{elec}} \quad (5)$$

The COMPASS force field cannot be used to calculate the $E_{\text{coh,H}}$ and $E_{\text{coh,P}}$ separately, but includes the two interactions in the E_{elec} as follows:

$$E_{\text{elec}} = E_{\text{coh,P}} + E_{\text{coh,H}} \quad (6)$$

In fact, to improve the calculation accuracy, most high-precision ab initio force fields do not have a separate hydrogen bond term. Only some old force field expressions such as Dreiding give a separate hydrogen bond term based on empirical and semiempirical force field parameters.⁴⁴ Then the solubility parameters can be given based on eqs 5 and 6:

$$\delta_{\text{T}}^2 = \delta_{\text{vdW}}^2 + \delta_{\text{elec}}^2 \quad (7)$$

$$\delta_{\text{elec}}^2 = \delta_{\text{p}}^2 + \delta_{\text{H}}^2 \quad (8)$$

Therefore, three-component Hansen solubility parameters (δ_{D} , δ_{p} , δ_{H}) are transformed into two-component solubility parameters (δ_{vdW} , δ_{elec}). In the work of Gupta⁴¹ and Lee,³⁴ similar two-component solubility parameters were involved. In this work, we calculated two-component solubility parameters of SWCNTs and polymers and investigated whether the two-component solubility parameters can predict their compatibility.

Model and Simulation Details. To explore the general rule of the relation between two-component solubility parameters and compatibility, six typical polymers were selected: PE, PS, PVC, NR, NBR, and EP. Their chemical formulas are shown in Figure 1. The mass fraction of acrylonitrile and butadiene in NBR is 41% and 59%, respectively. This simulated mass fraction is consistent with that of a commercial NBR product (N220S, Japan Synthetic

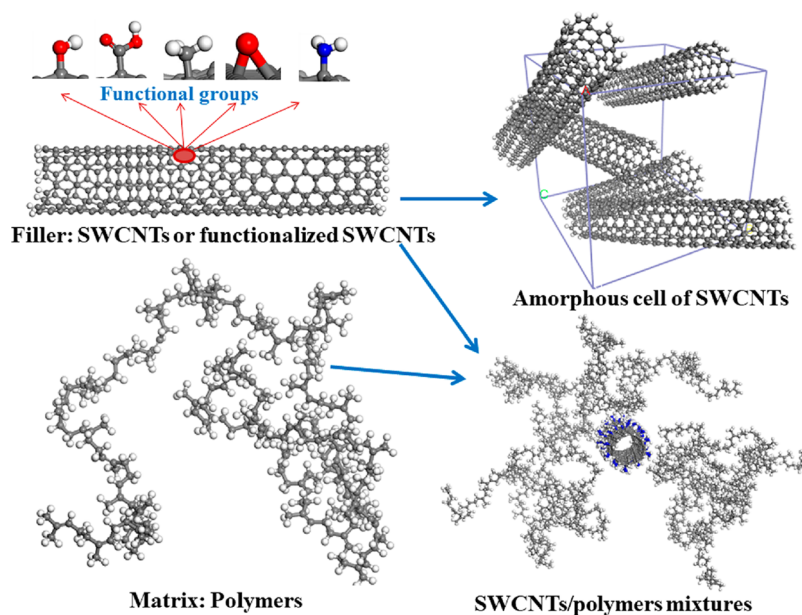


Figure 3. Amorphous cell consists of five SWCNTs and mixtures consist of polymeric chains as matrix and SWCNTs or functionalized SWCNTs as filler (gray, white, red, and blue balls represent C, H, O, and N atoms, respectively).

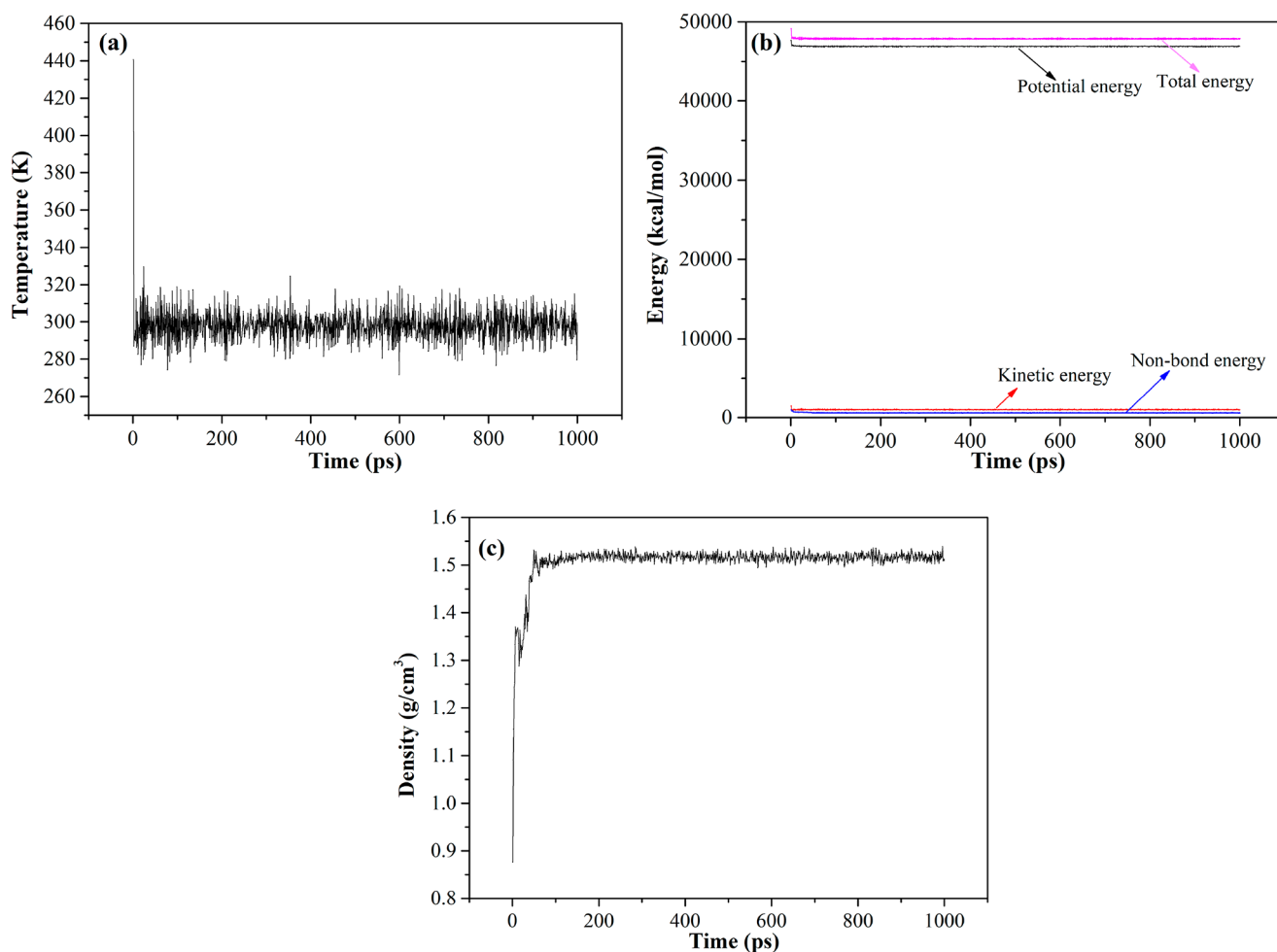


Figure 4. (a) Temperature, (b) energy, and (c) density as a function of time.

Rubber Co., Ltd.).⁴⁵ Each polymer chain model consists of 50 repeat units, i.e., the degree of polymerization, n , of 50. The amorphous cells containing 10 polymer chains were con-

structed to calculate the solubility parameters of polymers, as shown in Figure 2. The model of SWCNTs with a length of 40.64 Å and a diameter of 7.47 Å was constructed and the

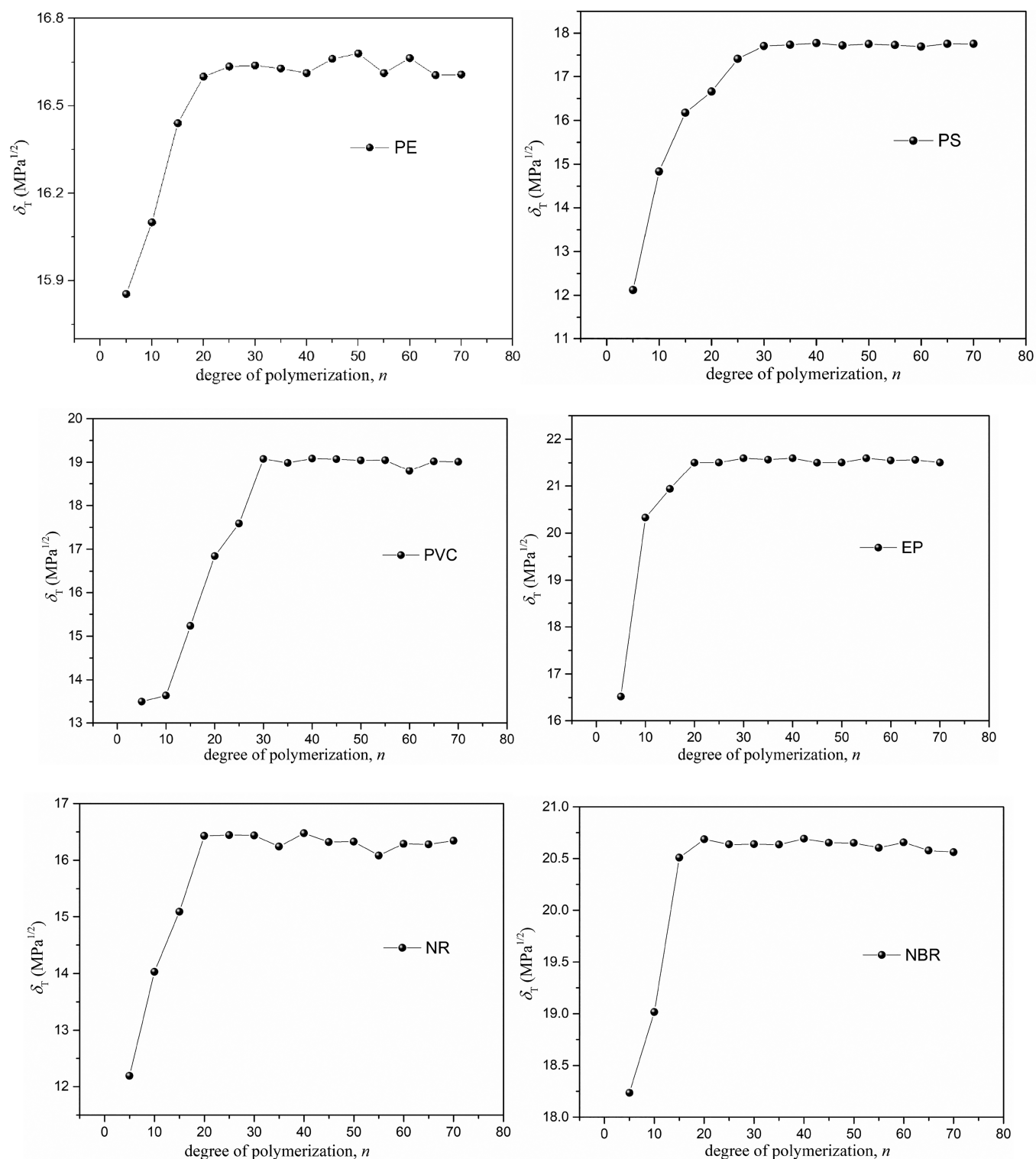


Figure 5. Solubility parameters of PE, PS, PVC, EP, NR, and NBR as a function of degree of polymerization.

unsaturated carbon atoms at the boundary were neutralized by hydrogenation. The size of CNTs in simulation is far less than the real size, and the unsaturated boundary effect is not ignorable in simulation. Therefore, the hydrotreating at the edge of CNTs is essential to maintain an electrically neutral system. A nanotube is formed by rolling a graphene sheet into a cylinder. Its structure can be uniquely characterized by defining the indices N and M of the chiral vector. N controls the overall size of the nanotube, and M controls the chiral

angle, or twist, of the graphite sheet used to construct the nanotube. The chirality vector (N,M) of pristine SWCNTs is (6,5). The $-\text{OH}$, $-\text{NH}_2$, $-\text{CH}_3$, $-\text{COOH}$, and $-\text{CH}(\text{O})-\text{CH}-$ groups were introduced into SWCNTs randomly to obtain the functionalized SWCNTs. Then the amorphous cells containing five SWCNTs or functionalized SWCNTs were constructed to calculate their solubility parameter. The models of functionalized SWCNTs and the amorphous cell of SWCNTs are shown in Figure 3.

Table 1. Simulated and Experimental δ_T and ρ of Polymers As Well As the Simulated δ_T of SWCNTs^a

	δ_T (MPa ^{1/2}) _s	δ_{vdW} (MPa ^{1/2}) _s	δ_{elec} (MPa ^{1/2}) _s	δ_T (MPa ^{1/2}) _e	ρ (g/cm ³) _s	ρ (g/cm ³) _e	ref.
PE	16.6	16.2	0.6	16.3	0.91	0.89–0.93	18
PS	17.7	16.7	3.4	17.6	1.05	1.04–1.08	18
PVC	19.1	17.9	6.7	19.5	1.27	1.19–1.35	18
EP	21.5	18.1	8.3	22.1	1.32	1.10–1.40	18
NR	16.3	15.8	1.1	16.5	0.93	0.92–0.95	18
NBR	20.8	18.5	8.0	21.1	1.04	1.06	45
Pristine SWCNTs	26.0	25.6	0.4				

^aSubscript s represents the simulated value and e represents the experimental value.

In the calculation of solubility parameters, three-dimensional periodic boundary conditions were employed, and the initial densities of amorphous cells of polymers and SWCNTs were set to 1.0 and 0.6 g/cm³, respectively. The geometry optimization procedure with a Smart algorithm and energy convergence tolerance of 10⁻⁴ kcal/mol was first applied to the amorphous cell. The annealing procedure with five annealing cycles and 10 heating ramps per cycle from an initial temperature of 300 K to midcycle temperature of 800 K was then performed. After annealing, the geometry optimization procedure was performed once again. Finally, the amorphous cell was subjected to 1 ns of NVT (constant number of atoms, volume, and temperature) ensemble with 298 K and 1 ns of NPT (constant number of atoms, volume, and energy) ensemble with 298 K and one bar pressure to obtain equilibrium state. The solubility parameters of polymers and SWCNTs were calculated based on the results of the NPT ensemble. In all the simulations, the temperature was adjusted by Nosé thermostat, and the pressure was controlled by Berendsen barostat. The van der Waals interactions were calculated by Lennard–Jones (9–6) potential with a cutoff distance of 12.5 Å and the electrostatic interactions were calculated by the Ewald summation method with an Ewald accuracy of 10⁻⁴ kcal/mol. Newton's equation of motion was solved by Verlet velocity integration method with a time step of 1 fs.

The compatibility between SWCNTs and polymers was predicted by the Flory–Huggins model which is the best-known theory of the thermodynamics of mixing and phase separation in binary systems.⁴⁶ The Flory–Huggins model expression is given in the section on [Compatibility between Functionalized SWCNTs and Polymers](#). The Flory–Huggins parameter, χ , was calculated to describe the compatibility by the model of SWCNTs/polymers mixtures (see [Figure 3](#)). All modeling and simulation were performed using Materials Studio 7.0 software with COMPASS force field.

To prove that the system reaches the equilibrium state after 1 ns of NPT, the temperature, energy, and density as a function of time are given in [Figure 4](#). These parameters are stable at 1 ns indicating that the system reaches the equilibrium state.

Besides, to verify the validity of the polymer models, we investigated the δ_T of polymers as a function of the degree of polymerization, as shown in [Figure 5](#). All these results show that as the degree of polymerization increases, the δ_T of polymer first increases rapidly and then remains stable at a certain degree of polymerization. In general, the degree of polymerization corresponding to the stable δ_T can be used to describe the real polymer chain.^{19,47} Therefore, the degree of polymerization was set to 50. [Table 1](#) lists the simulated and experimental δ_T and density (ρ) of polymers as well as the

simulated δ_T of SWCNTs. The experimental solubility parameters of SWCNTs from some literature are presented in [Table 2](#). It is found that the simulated δ_T and ρ of polymers

Table 2. Experimental Solubility Parameters of SWCNTs from Literature^a

preparation methods	δ_T (MPa ^{1/2})	δ_D (MPa ^{1/2})	δ_P (MPa ^{1/2})	δ_{H1} (MPa ^{1/2})	ref.
WCVD	18.1	16.4	7.5	4.0	23
HiPCO	20.8	17.8	7.5	7.6	24
CCVD	(24.9) ^a	17.4	13.7	11.3	48
CCVD	(26.8) ^a	19.4	10.4	15.2	49
WCVD	26.5	22.1	11.3	9.1	31
CCVD	(21.0) ^a	19.5	6.5	4.5	50
HiPCO	(20.6) ^a	18.0	7.4	6.8	51

^aNot presented, but calculated from [eq 3](#). WCVD (water-assisted chemical vapor deposition), CCVD (combustion chemical vapor deposition), and HiPCO (high-pressure CO conversion).

are in good agreement with the experimental values, which indicates the reliability of the simulation. However, the SWCNTs prepared by different methods have different solubility parameters, and the simulated δ_T of 26.0 MPa^{1/2} is different from the experimental values. Note that the pristine finite-length SWCNTs without any defects and functional groups were constructed in the simulation. But the real experimental CNTs are not guaranteed to be completely single-walled, and functional groups and defects are inevitable.³⁰ The previous experiment also indicated that the length and diameter of SWCNTs can affect the solubility parameter.²³ Therefore, the factors affecting the solubility parameter of CNTs and the reason for the difference between the simulated and experimental solubility parameters are considered to be mainly the following four aspects: (1) defect, (2) aspect ratio, (3) the number of walls, and (4) functional group.

RESULTS AND DISCUSSION

Effect of the SWCNTs Agglomeration on the Solubility Parameters. Here the effect of the SWCNTs agglomeration on the solubility parameters was studied. Because there are five SWCNTs in the amorphous cell, we considered two types of agglomeration: (a) two SWCNTs agglomerated to form two aggregates and (b) three SWCNTs agglomerated to form three aggregates. Two types of agglomeration and four amorphous cells with different agglomerated morphologies are shown in [Figure 6](#). Therefore, four amorphous cells with different agglomerated morphologies were constructed: (c) Aggregate 1: three aggregates + two aggregates, (d) Aggregates 2: three aggregates, (e) Aggregates

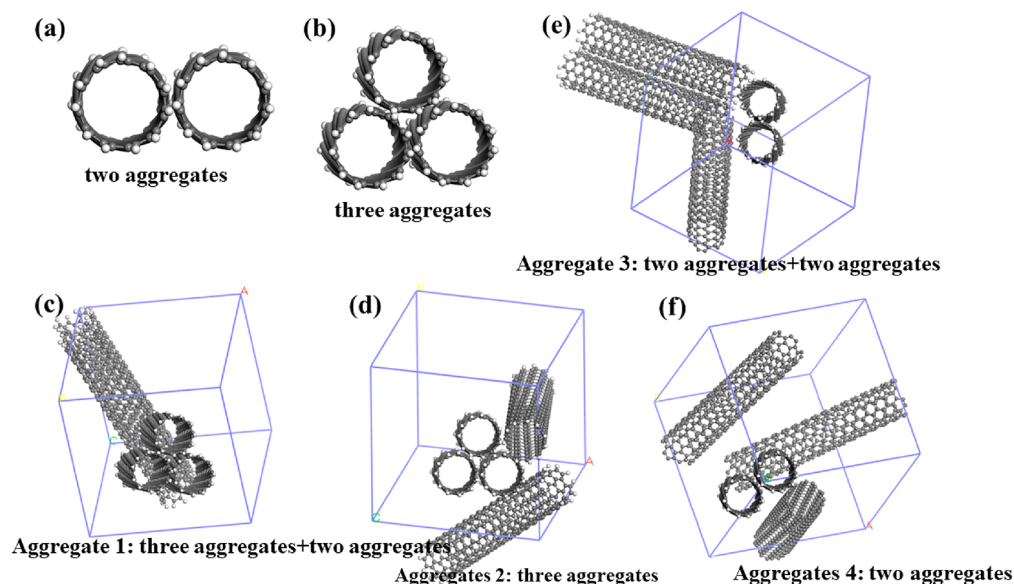


Figure 6. Two types of agglomeration, (a) two aggregates and (b) three aggregates, and four amorphous cells with different agglomerated morphologies, (c) Aggregate 1: three aggregates + two aggregates, (d) Aggregate 2: three aggregates, (e) Aggregate 3: two aggregates+two aggregates, and (f) Aggregate 4: two aggregates.

3: two aggregates+two aggregates, and (f) Aggregates 4: two aggregates. As shown in Figure 7, the more serious the agglomeration, the smaller the solubility parameter.

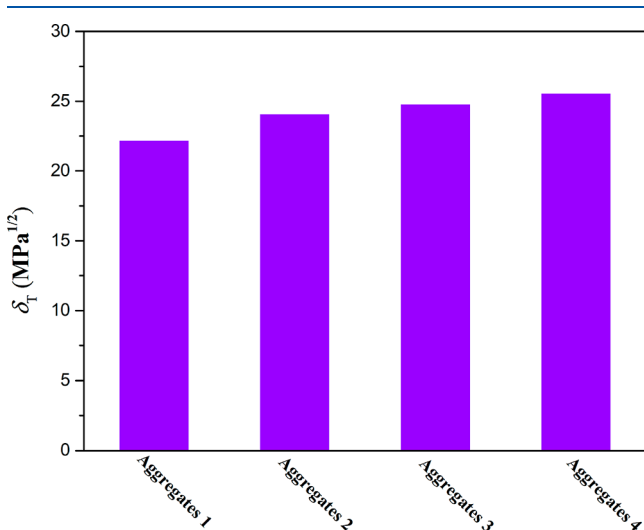


Figure 7. Effect of the SWCNTs agglomeration on the solubility parameters.

Solubility Parameters of Defective SWCNTs. The vacancy and Throrer–Stone–Wales (TSW) defects in graphite lattice of CNTs are the two most concerned defects.^{11,12} The graphite lattice misses one carbon atom to form the monovacancy defect and misses two adjacent carbon atoms to form the divacancy defect, as shown in Figure 8. Besides, the hexagonal graphite lattice can be reconstructed under external conditions (e.g., high temperature or electric field).⁵² Such as, four hexagons are transformed into two pentagons and two heptagons by rotating a C–C bond by 90° without the miss of carbon atoms, which is TSW (55–77) defect (see Figure 8d). The reconstruction of monovacancy can form a pentagon and a nonagon (monovacancy 5–9) and

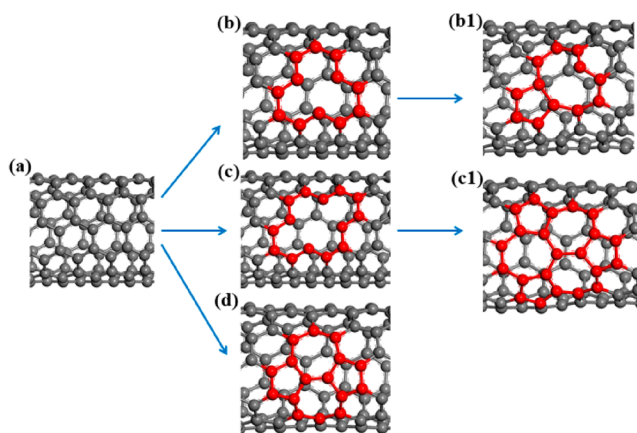


Figure 8. Type of defects: (a) pristine CNTs, (b) monovacancy, (c) divacancy, and (d) TSW (55–77). Reconstructed (b1) monovacancy (5–9) and (c1) divacancy (55–777) defects.

the reconstruction of bivacancy can form three pentagons and three heptagons (divacancy 555–777), as shown in Figure 8b1 and c1.

The nonbond energies of pristine SWCNTs and SWCNTs with different types of defects are listed in Table 3. The decrease of E_{vdW} and the increase of E_{ele} with increase of the number of missing carbon atom are found. The increase of E_{ele} is attributed to the formation of dangling bond by missing carbon atom. However, the decrease effect is larger than the

Table 3. Non-Bond Energies of SWCNTs with Different Types of Defects

types of defects	E_{vdW} (kcal/mol)	E_{ele} (kcal/mol)	$E_{nonbond}$ (kcal/mol)
pristine SWCNTs	1096.407	135.669	1232.076
monovacancy	1083.513	124.185	1207.698
divacancy	1017.311	125.916	1142.637
TSW	1105.589	132.326	1237.915

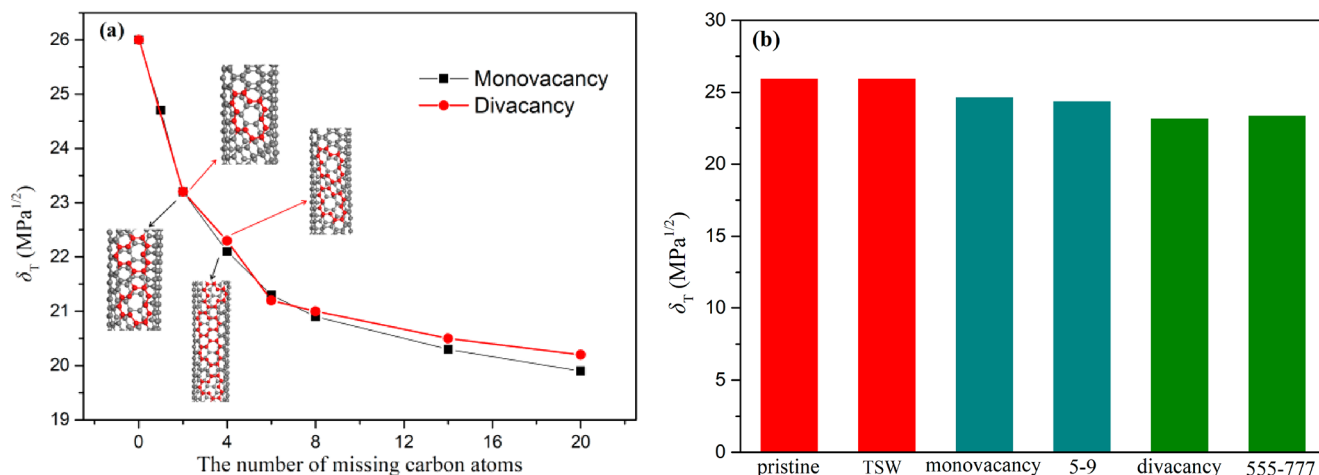


Figure 9. Effect of (a) missing carbon atoms and (b) defect reconstruction on the solubility parameter.

increase effect, leading to the decrease of E_{nonbond} . The SWCNTs with TSW defect from lattice reconstruction has a similar E_{nonbond} with the pristine SWCNTs.

The effect of defect type and reconstruction on the solubility parameter of SWCNTs is shown in Figure 9. The solubility parameters of SWCNTs with monovacancy and divacancy defects are nearly identical at the same number of missing carbon atoms. As the number of missing carbon atoms increases, the solubility parameter decreases significantly. Such as when the number of missing carbon atoms is 20, the solubility parameter decreases from 26.0 to 20.0 MPa^{1/2}, a decrease of 23.1%. From Figure 9b, the reconstruction has little effect on the solubility parameter of SWCNTs. In conclusion, the defect has a great effect on the solubility parameter of SWCNTs, and the solubility parameter is only related to the number of missing carbon atoms.

Effect of the Size and Chirality of SWCNTs on Solubility Parameters. We constructed 10 SWCNTs with different lengths and diameters to investigate the effect of the size on the solubility parameter, as listed in Table 4. The samples no. 1–7 keep constant diameter and the samples no. 8–12 keep constant length. It is found that as the length increases, the solubility parameter changes little, but as the diameter increases, the solubility parameter decreases

Table 4. Solubility Parameter for SWCNTs as a Function of Length and Diameter^a

sample no.	length (Å)	diameter (Å)	aspect ratio (length/diameter)	δ_T (MPa ^{1/2})
1	14.94	7.47	2.0	26.7
2	22.41	7.47	3.0	27.1
3	29.88	7.47	4.0	26.2
4	37.35	7.47	5.0	26.3
5	44.82	7.47	6.0	26.5
6	52.29	7.47	7.0	26.2
7	59.76	7.47	8.0	26.1
8	40.63	5.13	7.9	28.3
9	40.63	5.65	7.2	27.4
10	40.63	6.21	6.5	26.8
11	40.63	6.83	5.9	26.5
12	40.63	7.47	5.4	26.0

^aSamples No. 1–7 keep constant diameter and samples No. 8–12 keep constant length.

obviously (see Figure 10). Understandably, an increase in diameter will result in a reduction in the number of carbon

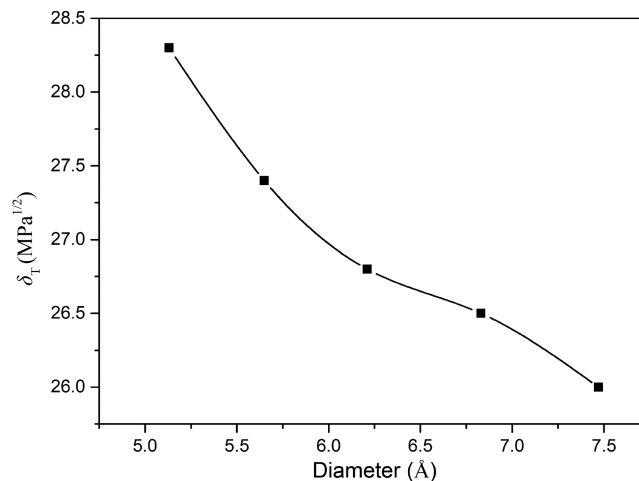


Figure 10. Solubility parameters of SWCNTs as a function of diameter.

atoms per unit volume, which will reduce the intermolecular interactions or CED and thus the solubility parameter.³⁴

To explore the effect of the chirality on solubility parameters of SWCNTs, we constructed four kinds of finite-length models of SWCNTs with different chirality: (a) (6,5), (b) (9,1), (c) (10,0) zigzag, and (d) (5,5) armchair, as shown in Figure 11. Their diameter, length, and solubility parameters are listed in Table 5. It is found that the δ_T values of (6,5) and (9,1) SWCNTs are the same, which is attributed to the same length and diameter. Besides the δ_T of (10,0) zigzag SWCNT is lower than that of (5,5) armchair SWCNT.

Effect of the Number of Walls on Solubility Parameters of CNTs. The solubility parameters of CNTs with the number of walls from 1 to 10 were investigated. The model of CNTs with 10 walls is shown in Figure 12a, and the wall separation is $d = 3.347$ Å. This result is presented in Figure 12b. As the number of walls increases, the solubility parameter within 3 or 4 walls increases dramatically, and then increases slowly. Lee et al.³⁴ investigated the solubility parameters of SWCNTs and double-walled carbon nanotubes (DWCNTs) and found that the solubility parameter of

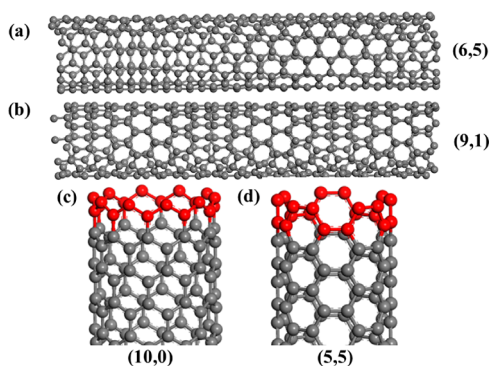


Figure 11. Finite-length model of SWCNTs with different chirality: (a) (6,5), (b) (9,1), (c) (10,0) zigzag, and (d) (5,5) armchair. The hydrogen atoms are omitted for display.

Table 5. Solubility Parameters of SWCNTs with Different Chirality

(N,M)	diameter (Å)	length (Å)	δ_T (MPa ^{1/2})
(6,5)	7.47	40.64	26.0
(9,1)	7.47	40.64	26.0
(10,0)	7.83	42.60	25.4
(5,5)	6.78	41.81	26.8

DWCNTs is greater than that of SWCNTs. Besides, they guessed that increasing the number of walls will increase the solubility parameter of CNTs. Our study here confirms their guess. Lee et al.³⁴ believed that the effect of the number of walls on the solubility parameter is related to the cutoff distance of van der Waals interactions. The cutoff distance of 12.5 Å in this simulation shows that when the distance between atoms exceeds 12.5 Å, the pair interactions are negligible. For another, the wall separation of 3.347 Å suggests that only the first three or four outer walls actually participate in the intermolecular interactions ($3 \times 3.347 \text{ Å} < 12.5 \text{ Å} < 4 \times 3.347 \text{ Å}$). Therefore, the number of walls has a significant effect on the solubility parameters within 3 or 4 walls, while as the number of walls continues to increase, the effect of the number of walls is slight.

Solubility Parameters of Functionalized SWCNTs. We systematically investigated Hildebrand and two-component solubility parameters of $-\text{OH}$, $-\text{CH}(\text{O})\text{CH}-$, $-\text{NH}_2$, $-\text{COOH}$, and $-\text{CH}_3$ functionalized SWCNTs as a function of grafting ratio, as shown in Figure 13. The grafting ratio of functional groups is defined as follows:

$$\text{grafting ratio} = \frac{n}{N} \times 100 \quad (9)$$

where n is the number of functional groups and $N = 364$ is the number of carbon atoms in SWCNTs. In the simulation, the maximum grafting ratio is set to 25.0%. Interestingly, no matter which group is grafted, the δ_T and δ_{vdW} have the same change trend. That is, as the grafting ratio increases, the δ_T and δ_{vdW} decrease first, reach a minimum at a certain grafting ratio, and then increase. Our previous study on the solubility parameter of graphene as a function of grafting ratio also found the same law and the reason for this law was explored.⁵³ Briefly, in the initial stage, as the grafting ratio increases, the increasing effect of van der Waals and electrostatic interactions is less than the decreasing effect of $\pi-\pi$ stacking interactions, resulting in a decrease in δ_T and δ_{vdW} . The increasing effect exactly offsets the decreasing effect at a certain grafting ratio, so the solubility parameter has a minimum. As the grafting ratio continues to increase, the increasing effect exceeds the decreasing effect so that the solubility parameter increases. Therefore, the competitive effect of $\pi-\pi$ stacking, van der Waals and electrostatic interactions are the reason for a minimum δ_T or δ_{vdW} at a certain grafting ratio. Besides the solubility parameters of SWCNTs and graphene are compared in Supporting Information (SI). The δ_{elec} first increases rapidly and then slowly with grafting ratio. The magnitude of δ_{elec} of functionalized SWCNTs with different functional groups is $-\text{COOH} > -\text{OH} > -\text{NH}_2 > -\text{CH}(\text{O})\text{CH}- > -\text{CH}_3$. The δ_{elec} has been proven to be related to the charge per unit volume, that is, charge density.⁵³

It is worth noting that the minimum δ_T or δ_{vdW} is very crucial for the functionalization of SWCNTs, which determines the degree of compatibility between functionalized SWCNTs and polymers. The minimum δ_T and the corresponding grafting ratio are presented in Figure 14. The minimum δ_T values of $-\text{OH}$, $-\text{NH}_2$, $-\text{CH}_3$, $-\text{COOH}$, and $-\text{CH}(\text{O})\text{CH}-$

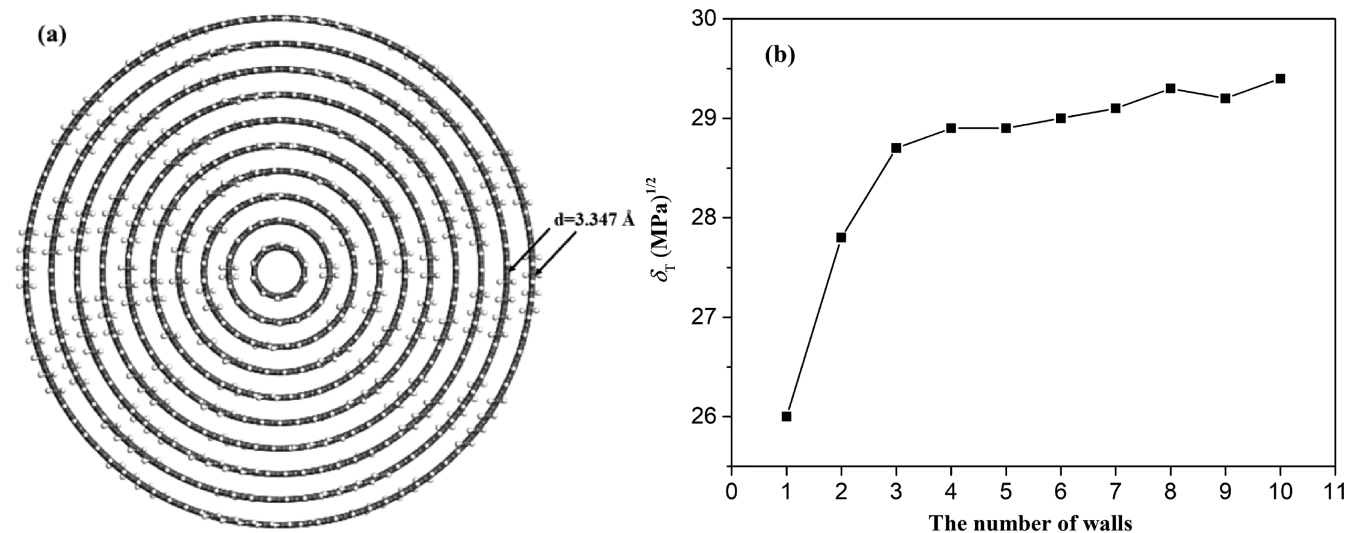


Figure 12. (a) The model of CNTs with 10 walls and (b) the δ_T of CNTs with the number of walls from 1 to 10.

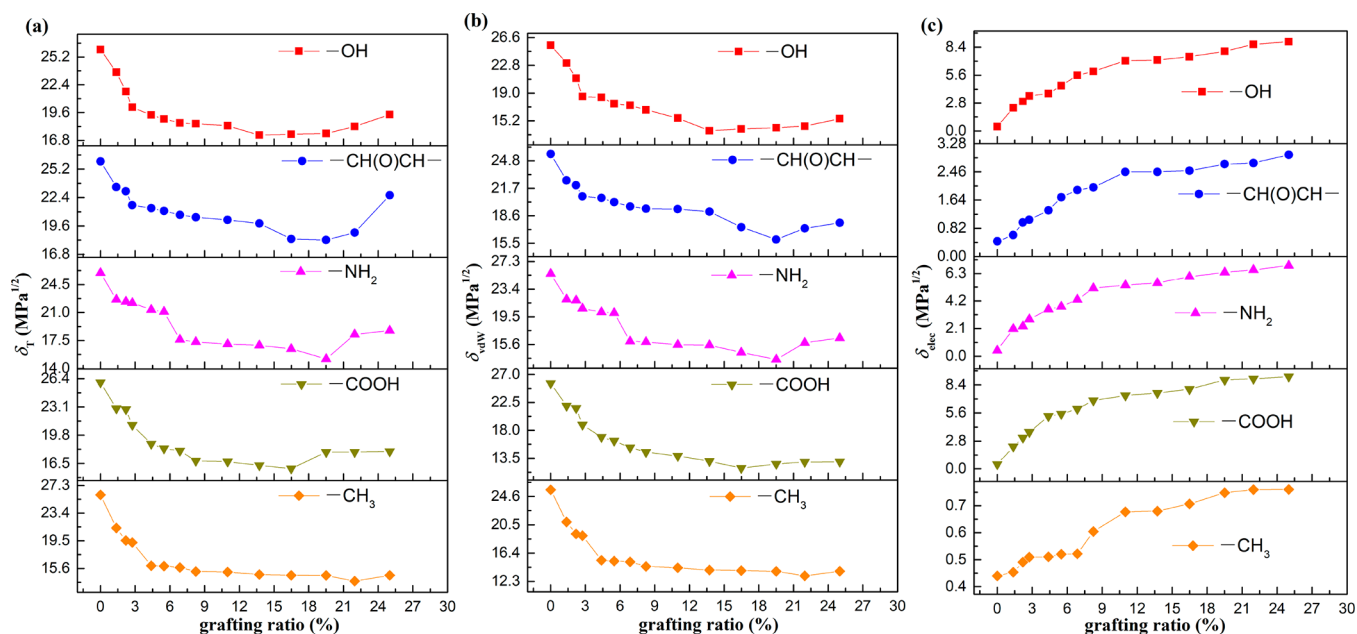


Figure 13. Solubility parameters of $-\text{OH}$, $-\text{CH}(\text{O})\text{CH}-$, $-\text{NH}_2$, $-\text{COOH}$ and $-\text{CH}_3$ functionalized SWCNTs as a function of grafting ratio: (a) Hildebrand solubility parameters (δ_T) and two-component solubility parameters including (b) van der Waals (δ_{vdW}) and (c) electrostatic (δ_{ele}) components.

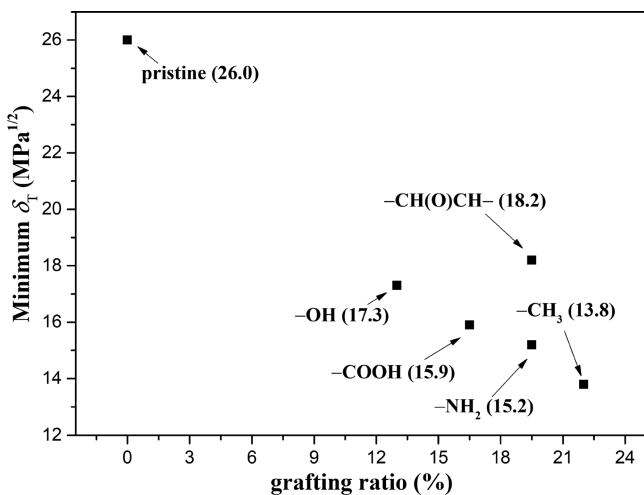


Figure 14. Minimum δ_T and corresponding grafting ratio (the minimum δ_T is presented in brackets). To facilitate the display, we employ functional groups to express the functionalized SWCNTs here.

functionalized SWCNTs decrease by 33.4%, 41.4%, 46.9%, 38.8%, and 29.9%, respectively, compared with the δ_T of pristine SWCNTs. This shows that the functional groups have a significant effect on the solubility parameters. In addition, the minimum δ_T of functionalized SWCNTs and the δ_T of polymers are sorted as follows: EP > NBR > PVC > $-\text{CH}(\text{O})\text{CH}-$ > PS > $-\text{OH}$ > PE > NR > $-\text{COOH}$ > $-\text{NH}_2$ > $-\text{CH}_3$. To facilitate the display, we employ functional groups to express the functionalized SWCNTs here. The order of solubility parameters will make the polymers and functionalized SWCNTs exhibit different compatible behaviors. This will be elaborated in the section on **Compatibility between functionalized SWCNTs and Polymers**.

Returning to Tables 1 and 2, the simulated and the experimental δ_T values have some differences. The studies

above show that the solubility parameter of CNTs will be reduced by increasing defects, functional groups, and diameters, while the solubility parameter will be increased by increasing the number of walls. Therefore, we speculate that the competitive effect of these factors may result in the difference between the simulated and the experimental δ_T .

Compatibility between Functionalized SWCNTs and Polymers. Two-component solubility parameters of polymers and functionalized SWCNTs have been obtained in the above sections. Then whether two-component solubility parameters can be used to predict their compatibility effectively is the focus here. In the theory of mixing thermodynamic, the Gibbs free energy of mixing (ΔG_{mix}) composed of enthalpy (ΔH_{mix}) and entropy (ΔS_{mix}) of mixing determines the compatible behavior of two components.¹⁸

$$\Delta G_m = \Delta H_m - T\Delta S_m \quad (10)$$

where T is the absolute temperature. The negative ΔG_{mix} indicates a good spontaneous compatibility between components A and B. When two components are mixed, ΔS_{mix} is commonly positive. So to ensure that ΔG_{mix} is negative, ΔH_{mix} needs to be as small as possible. The best-known theory of the thermodynamics of mixing and phase separation in binary systems is the Flory–Huggins model in which ΔH_{mix} can be expressed by the following:⁴⁴

$$\Delta H_m = \frac{\chi\varphi_A\varphi_B kT}{V_0} \quad (11)$$

where φ_A and φ_B are volume fraction of component A as solvent and component B as a solute, k is the Boltzmann constant, and V_0 is the molecular volume (lattice site volume in the lattice theory) of component A. Besides, Hildebrand and Scatchard also proposed the ΔH_{mix} expression as follows:⁵⁴

$$\Delta H_m = \varphi_A\varphi_B(\delta_{T,A} - \delta_{T,B})^2 V_M \quad (12)$$

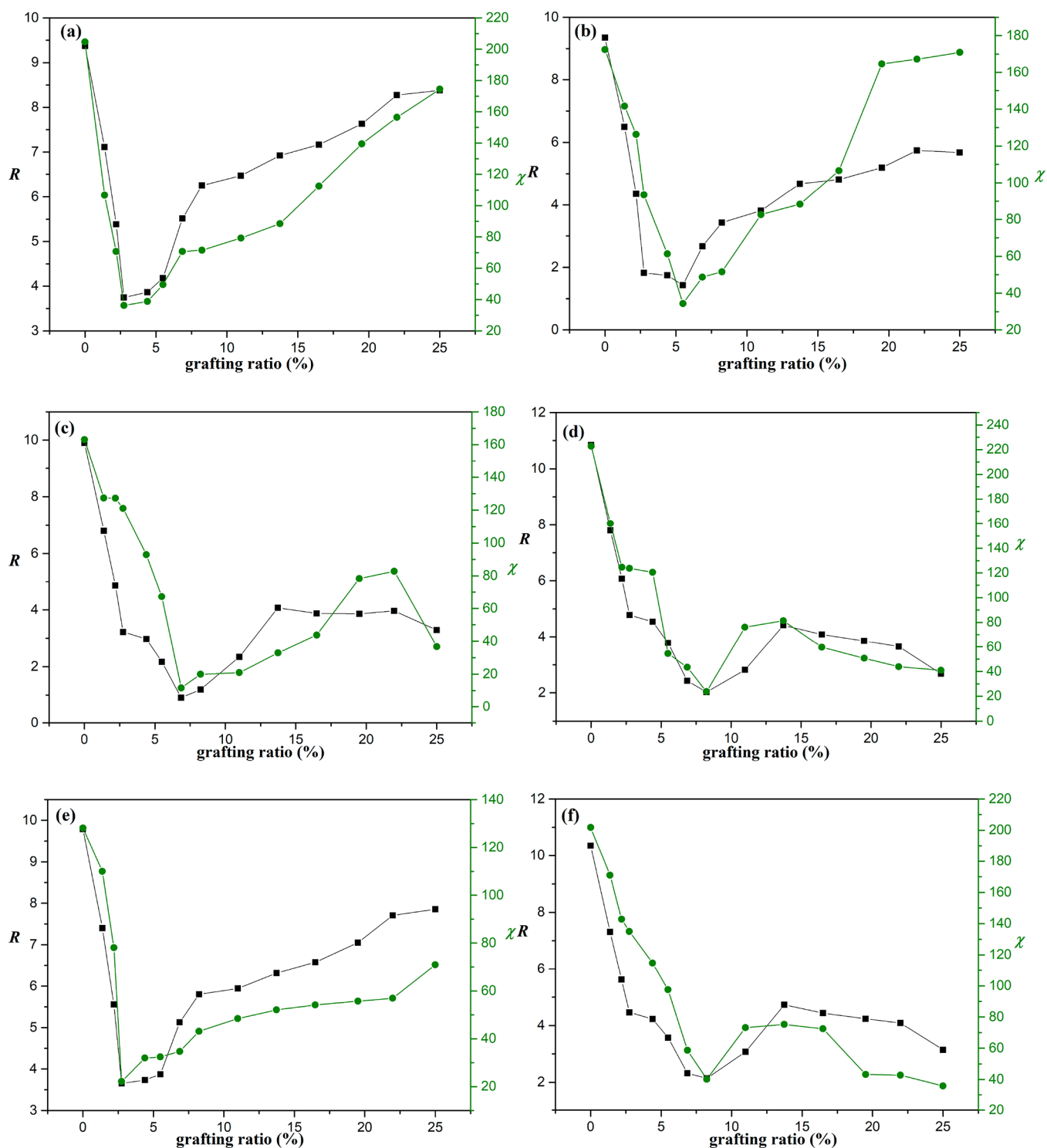


Figure 15. R and χ as a function of grafting ratio in $-\text{OH}$ functionalized SWCNTs/polymers mixtures: (a) PE, (b) PS, (c) PVC, (d) EP, (e) NR, and (f) NBR.

where V_M is the total volume after mixing, and $\delta_{T,A}$ and $\delta_{T,B}$ are the Hildebrand solubility parameters of components A and B, respectively. According to eqs 11 and 12, the relationship between χ and δ is as follows:

$$\chi = \frac{V_0 V_M}{kT} (\delta_{T,A} - \delta_{T,B})^2 \quad (13)$$

Therefore, only when the δ is close or the χ value is small, can ΔH_{mix} be as small as possible to ensure a negative ΔG_{mix} value

and a good compatibility. On the basis of eq 13, Hansen further replaced the Hildebrand solubility parameter with the Hansen solubility parameters as follows:¹⁸

$$\chi = \frac{V_0 V_M}{kT} [(\delta_{D,A} - \delta_{D,B})^2 + (\delta_{P,A} - \delta_{P,B})^2 + (\delta_{H,A} - \delta_{H,B})^2] \quad (14)$$

Then a simple parameter, R_0 , was proposed to describe the proximity of the solubility parameters of component A and B as follows:

$$R_0 = [(\delta_{D,A} - \delta_{D,B})^2 + (\delta_{P,A} - \delta_{P,B})^2 + (\delta_{H,A} - \delta_{H,B})^2]^{1/2} \quad (15)$$

The smaller R_0 denotes the closer Hansen solubility parameters. Similarly, we replaced Hansen solubility parameters with two-component solubility parameters of SWCNTs and polymers, and a parameter, R , is given by the following:

$$R = [(\delta_{vdW,polymer} - \delta_{vdW,SWCNTs})^2 + (\delta_{elec,polymer} - \delta_{elec,SWCNTs})^2]^{1/2} \quad (16)$$

where $\delta_{polymer}$ and δ_{SWCNTs} are the solubility parameters of polymer and SWCNTs, respectively. Therefore, to know whether two-component solubility parameters can describe the compatibility between SWCNTs and polymers, the R and χ values need to be compared. If R is proportional to χ , then it turns out that two-component solubility parameters can describe effectively the compatibility, but the opposite is not. The χ value of binary systems can be obtained by the Flory–Huggins model as follows:⁵⁴

$$E_{mix} = \frac{1}{2}Z(E_{bs} + E_{sb} - E_{bb} - E_{ss}) \quad (17)$$

$$\chi = \frac{E_{mix}}{R_u T} \quad (18)$$

where E_{mix} is the mixing energy of binary systems, E_{ij} ($i, j = s$ or b) is the binding energy between a unit of component i and a unit of component j , and R_u is the universal gas constant.

The R and χ values of 30 mixture systems (six polymers and five functional groups) were calculated and as an example, R and χ as a function of grafting ratio in –OH functionalized SWCNTs/polymers mixtures are presented in Figure 15. Other groups functionalized SWCNTs/polymers mixtures are presented in the SI. These results show that R is proportional to χ for each mixture. That is, two-component solubility parameters are proven to be able to effectively predict the compatibility between SWCNTs and polymers. Besides, two types of compatibility behaviors between functionalized SWCNTs and polymers are found. One is that as the grafting ratio increases, R or χ first decreases, reaches a minimum, and then increases. This type of curve is V-shaped, such as for –OH functionalized SWCNTs/PE mixture (see Figure 15a). The other is that the variation of R along the grafting ratio is of W-shape, such as for –NH₂ functionalized SWCNTs/PE mixture (see Figure S1a). The order of the δ_T of polymers and the minimum δ_T of functionalized SWCNTs determine the above results. For example, the minimum δ_T (17.3 MPa^{1/2}) of –OH functionalized SWCNTs is larger than the δ_T (16.6 MPa^{1/2}) of PE, so there is a minimum R with increasing grafting ratio. For another, the minimum δ_T (15.2 MPa^{1/2}) of –NH₂ functionalized SWCNTs is lower than the δ_T of PE, so R has two minima (W-shape). In some mixtures such as –OH functionalized SWCNTs/PVC mixture, the W-shape is not complete. We speculate that this is because the grafting ratio is not high enough. When the grafting ratio continues to increase, the curve will show a complete W-shape. Therefore the incomplete W-shape is also classified as W-shape. The compatibility behavior, i.e., the shape of the curve for R with grafting ratio is listed in Table 6. It is found that the curves for polymer systems with high polarity (PVC, EP, and NR) are of W-shape. This is because these polar polymers have high solubility parameters. The solubility parameters of polymers with low polarity (PE, PS, and NR) are not high, so the curve may be V-shaped or W-shaped.

Table 6. Compatibility Behavior of Functionalized SWCNTs and Polymers^a

	PE	PS	PVC	EP	NR	NBR
–OH	V	V	W	W	V	W
–NH ₂	W	W	W	W	W	W
–CH ₃	W	W	W	W	W	W
–COOH	V	W	W	W	V	W
–CH(O)CH–	V	V	W	W	V	W

^aV and W represent the curves of R with grafting ratio are V- and W-shaped, respectively.

Another important aspect is that the grafting ratio corresponding to the minimum R or χ is the so-called optimum grafting ratio at which the compatibility is the best. The optimum grafting ratios for different mixtures are listed in Table 7. We find that different mixtures have different optimum grafting ratios and the optimum grafting ratios for PVC, EP, and NR mixtures are relatively high. Some experiments have also shown that there is an optimum modification content for CNTs at which the CNTs dispersion is the best and the properties of CNTs/polymer composites are the optimum.¹⁰ Our study provides a theoretical insight into these experimental phenomena.

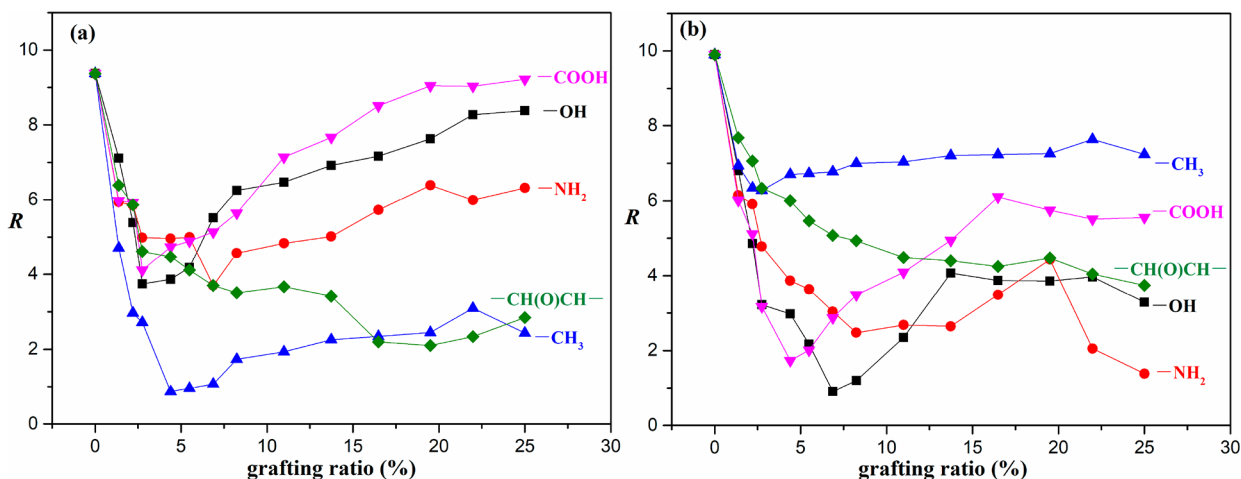
Functionalization Principle of SWCNTs. From the view of thermodynamics, the intrinsic properties of SWCNTs and SBR as well as their compatibility determine the properties of SWCNTs/polymers composites. The above study has shown that the functionalization of SWCNTs can improve the compatibility with polymers, but the introduction of functional groups also causes the properties of SWCNTs to decline due to the destruction of the graphite lattice.^{11,12} Therefore the functionalization principle of SWCNTs should be to improve the compatibility with polymers while maintaining the intrinsic properties of SWCNTs as much as possible. That is, the R or χ has a low value at a low grafting ratio. The R values of different functional groups with the grafting ratio for (a) PE and (b) PVC are presented in Figure 16. The R values for PS, EP, NR, and NBR systems are shown in Figure S5. Then the priority of the introduction of the functional group into SWCNTs is as follows from the view of compatibility between SWCNTs and PE: –CH₃ > –CH(O)CH– > –NH₂ > –OH > –COOH. However, the priority of the introduction of the functional group into SWCNTs for PVC with high polarity is different from that for PE with low polarity. The –CH₃ group has the last priority for PVC. In summary, different polymers show different functionalization principles. Polymers with low polarity should preferentially introduce the group that makes SWCNTs have low δ_{elec} , while polymers with high polarity should preferentially introduce the groups with makes SWCNTs have high δ_{elec} .

CONCLUSIONS

The effect of defects, size, the number of walls, and functional groups on Hildebrand and two-component solubility parameters of CNTs is investigated at the molecular level. The compatibility between functionalized SWCNTs and six typical polymers is elaborated by the Flory–Huggins model. The main conclusions are summarized in the following section. All the conclusions will provide helpful ideas to the understanding of basic physical properties of CNTs, the functionalization of SWCNTs, and the preparation of high-performance SWCNTs/polymers composites.

Table 7. Optimum Grafting Ratios of Different SWCNTs/Polymers Mixtures

	PE (%)	PS (%)	PVC (%)	EP (%)	NR (%)	NBR (%)
–OH	2.7	5.5	6.9	8.2	2.7	8.2
–NH ₂	6.9	6.9	25.0	25.0	6.9	25.0
–CH ₃	4.4	4.4	2.7	2.7	4.4	2.7
–COOH	2.7	4.4	4.4	4.4	2.7	4.4
–CH(O)CH–	19.5	22.0	25.0	25.0	16.5	25.0

Figure 16. *R* values of different functional groups with grafting ratio for (a) PE and (b) PVC.

- (i) Three-component Hansen solubility parameters are transformed into two-component solubility parameters based on the force field method. The δ_T of CNTs will be decreased by increasing defects and diameters, while the δ_T will be increased by increasing the number of walls. Two-component solubility parameters of polymers and functionalized SWCNTs were calculated. It is found for each functional group that as the grafting ratio increases, the δ_T and δ_{vdw} of SWCNTs decrease first, reach a minimum at a certain grafting ratio, and then increase. Additionally, the δ_{elec} of SWCNTs first increases rapidly and then slowly with grafting ratio.
- (ii) Two-component solubility parameters are proven to be able to predict effectively the compatibility between SWCNTs and polymers. There is an optimum grafting ratio at which the χ is the smallest, and the compatibility between SWCNTs and polymers is the best. Different mixtures have different optimum grafting ratios and the optimum grafting ratios for PVC, EP, and NR mixtures are relatively high.
- (iii) Two types of compatibility behaviors between functionalized SWCNTs and polymers are found. One is that as the grafting ratio increases, χ first decreases, reaches a minimum, and then increases. This type of curve is V-shaped. The other is that the variation of χ along the grafting ratio is of W-shape. From the view of thermodynamic compatibility, six polymers show different functionalization principles (the priority of the introduction of the functional group into SWCNTs).

ASSOCIATED CONTENT

Supporting Information

The Supporting Information is available free of charge at <https://pubs.acs.org/doi/10.1021/acs.langmuir.0c01736>.

Comparison of solubility parameters of SWCNTs and graphene, as well as *R* and χ as a function of grafting ratio (PDF)

AUTHOR INFORMATION

Corresponding Authors

Yanlong Luo – College of Science and Institute of Polymer Materials, Nanjing Forestry University, Nanjing 210037, P. R. China; orcid.org/0000-0002-7765-7911; Email: luoyanlong@njfu.edu.cn

Zhenyang Luo – College of Science and Institute of Polymer Materials, Nanjing Forestry University, Nanjing 210037, P. R. China; orcid.org/0000-0001-5063-2856; Email: luozhenyang@njfu.edu.cn

Authors

Xianling Chen – College of Science, Nanjing Forestry University, Nanjing 210037, P. R. China

Sizhu Wu – State Key Laboratory of Organic–Inorganic Composites, Beijing University of Chemical Technology, Beijing 100029, P. R. China; orcid.org/0000-0001-7863-2954

Songyuan Cao – College of Materials Science and Engineering, Nanjing Tech University, Nanjing 21009, P. R. China

Yijun Shi – Division of Machine Elements, Luleå University of Technology, 97187 Luleå, Sweden

Complete contact information is available at: <https://pubs.acs.org/doi/10.1021/acs.langmuir.0c01736>

Notes

The authors declare no competing financial interest.

ACKNOWLEDGMENTS

This work was supported by the National Natural Science Foundation of China (Grant No. 51903122), the start-up funds for the talents of Nanjing Forestry University

(No.163101128), and a project funded by the Priority Academic Program Development of Jiangsu Higher Education Institutions (PAPD).

REFERENCES

- (1) Tan, Y. S.; Liu, H.; Ruan, Q.; Wang, H.; Yang, J. K. W. Plasma-assisted filling electron beam lithography for high throughput patterning of large area closed polygon nanostructures. *Nanoscale* **2020**, *12*, 10584–10591.
- (2) Han, J.; Wang, H.; Yue, Y.; Mei, C.; Chen, J.; Huang, C.; Wu, Q.; Xu, X. A self-healable and highly flexible supercapacitor integrated by dynamically cross-linked electro-conductive hydrogels based on nanocellulose-templated carbon nanotubes embedded in a viscoelastic polymer network. *Carbon* **2019**, *149*, 1–18.
- (3) Yang, P.; Yang, L.; Gao, Q.; Luo, Q.; Zhao, X.; Mai, X.; Fu, Q.; Dong, M.; Wang, J.; Hao, Y.; Yang, R.; Lai, X.; Wu, S.; Shao, Q.; Ding, T.; Lin, J.; Guo, Z. Anchoring carbon nanotubes and post-hydroxylation treatment enhanced Ni nanofiber catalysts towards efficient hydrous hydrazine decomposition for effective hydrogen generation. *Chem. Commun.* **2019**, *55*, 9011–9014.
- (4) Dong, Q.; Nasir, M. Z. M.; Pumera, M. Semi-conducting single-walled carbon nanotubes are detrimental when compared to metallic single-walled carbon nanotubes for electrochemical applications. *Phys. Chem. Chem. Phys.* **2017**, *19*, 27320–27325.
- (5) Chen, J.; Cui, X.; Zhu, Y.; Jiang, W.; Sui, K. Design of superior conductive polymer composite with precisely controlling carbon nanotubes at the interface of a co-continuous polymer blend via a balance of pi-pi interactions and dipole-dipole interactions. *Carbon* **2017**, *114*, 441–448.
- (6) Zhang, H.; Zhang, G.; Tang, M.; Zhou, L.; Li, J.; Fan, X.; Shi, X.; Qin, J. Synergistic effect of carbon nanotube and graphene nanoplates on the mechanical, electrical and electromagnetic interference shielding properties of polymer composites and polymer composite foams. *Chem. Eng. J.* **2018**, *353*, 381–393.
- (7) Lu, Y.; Sun, D. X.; Qi, X. D.; Lei, Y. Z.; Yang, J. H.; Wang, Y. Achieving ultrahigh synergistic effect in enhancing conductive properties of polymer composites through constructing the hybrid network of 'rigid' submicron vapor grown carbon fibers and 'releable' carbon nanotubes. *Compos. Sci. Technol.* **2020**, *193*, 108141.
- (8) Song, S. H. Synergistic Effect of Clay Platelets and Carbon Nanotubes in Styrene-Butadiene Rubber Nanocomposites. *Macromol. Chem. Phys.* **2016**, *217*, 2617–2625.
- (9) Maity, K. P.; Patra, A.; Prasad, V. Influence of the chemical functionalization of carbon nanotubes on low temperature ac conductivity with polyaniline composites. *J. Phys. D: Appl. Phys.* **2020**, *53*, 125303.
- (10) Ma, P. C.; Siddiqui, N. A.; Marom, G.; Kim, J. K. Dispersion and functionalization of carbon nanotubes for polymer-based nanocomposites: A review. *Composites, Part A* **2010**, *41*, 1345–1367.
- (11) Dresselhaus, M. S.; Jorio, A.; Souza Filho, A. G.; Saito, R. Defect characterization in graphene and carbon nanotubes using Raman spectroscopy. *Philos. Trans. R. Soc., A* **2010**, *368*, 5355–5377.
- (12) He, X.; Hartmann, N. F.; Ma, X.; Kim, Y.; Ihly, R.; Blackburn, J. L.; Gao, W.; Kono, J.; Yomogida, Y.; Hirano, A.; Tanaka, T.; Kataura, H.; Htoon, H.; Doorn, S. K. Tunable room-temperature single-photon emission at telecom wavelengths from sp(3) defects in carbon nanotubes. *Nat. Photonics* **2017**, *11*, 577–582.
- (13) da Silva Ramos, A. C.; Rolemberg, M. P.; Moraes de Moura, L. G.; Zilio, E. L.; Pereira dos Santos, M. d. F.; Gonzalez, G. Determination of solubility parameters of oils and prediction of oil compatibility. *J. Pet. Sci. Eng.* **2013**, *102*, 36–40.
- (14) Santos, D. C.; Filipakis, S. D.; Lima, E. R. A.; Paredes, M. L. L. Solubility parameter of oils by several models and experimental oil compatibility data: implications for asphaltene stability. *Pet. Sci. Technol.* **2019**, *37*, 1596–1602.
- (15) Venkatram, S.; Kim, C.; Chandrasekaran, A.; Ramprasad, R. Critical Assessment of the Hildebrand and Hansen Solubility Parameters for Polymers. *J. Chem. Inf. Model.* **2019**, *59*, 4188–4194.
- (16) Belmares, M.; Blanco, M.; Goddard, W. A.; Ross, R. B.; Caldwell, G.; Chou, S. H.; Pham, J.; Olofson, P. M.; Thomas, C. Hildebrand and Hansen solubility parameters from molecular dynamics with applications to electronic nose polymer sensors. *J. Comput. Chem.* **2004**, *25*, 1814–1826.
- (17) Fang, X. H.; Li, B. Q.; Sokolov, J. C.; Rafailovich, M. H.; Gewaily, D. Hildebrand solubility parameters measurement via sessile drops evaporation. *Appl. Phys. Lett.* **2005**, *87*, No. 094103.
- (18) Hansen, C. M. *Hansen Solubility Parameters: A User's Handbook*, 2nd ed.; CRC Press: Boca Raton, FL, 2012.
- (19) Marsac, P. J.; Li, T.; Taylor, L. S. Estimation of Drug-Polymer Miscibility and Solubility in Amorphous Solid Dispersions Using Experimentally Determined Interaction Parameters. *Pharm. Res.* **2009**, *26*, 139–151.
- (20) Zhang, K.; Jia, N.; Li, S.; Liu, L. Millimeter to nanometer-scale tight oil-CO₂ solubility parameter and minimum miscibility pressure calculations. *Fuel* **2018**, *220*, 645–653.
- (21) Novo, L. P.; Curvelo, A. A. S. Hansen Solubility Parameters: A Tool for Solvent Selection for Organosolv Delignification. *Ind. Eng. Chem. Res.* **2019**, *58*, 14520–14527.
- (22) Hernandez, Y.; Lotya, M.; Rickard, D.; Bergin, S. D.; Coleman, J. N. Measurement of Multicomponent Solubility Parameters for Graphene Facilitates Solvent Discovery. *Langmuir* **2010**, *26*, 3208–3213.
- (23) Ata, S.; Mizuno, T.; Nishizawa, A.; Subramaniam, C.; Futaba, D. N.; Hata, K. Influence of matching solubility parameter of polymer matrix and CNT on electrical conductivity of CNT/rubber composite. *Sci. Rep.* **2015**, *4*, 7232.
- (24) Bergin, S. D.; Sun, Z.; Rickard, D.; Streich, P. V.; Hamilton, J. P.; Coleman, J. N. Multicomponent Solubility Parameters for Single-Walled Carbon Nanotube-Solvent Mixtures. *ACS Nano* **2009**, *3*, 2340–2350.
- (25) Ham, H. T.; Choi, Y. S.; Chung, I. J. An explanation of dispersion states of single-walled carbon nanotubes in solvents and aqueous surfactant solutions using solubility parameters. *J. Colloid Interface Sci.* **2005**, *286* (1), 216–223.
- (26) Lim, H. J.; Lee, K.; Cho, Y. S.; Kim, Y. S.; Kim, T.; Park, C. R. Experimental consideration of the Hansen solubility parameters of as-produced multi-walled carbon nanotubes by inverse gas chromatography. *Phys. Chem. Chem. Phys.* **2014**, *16*, 17466–17472.
- (27) Hansen, C. M.; Smith, A. L. Using Hansen solubility parameters to correlate solubility of C-60 fullerene in organic solvents and in polymers. *Carbon* **2004**, *42*, 1591–1597.
- (28) Launay, H.; Hansen, C. M.; Almdal, K. Hansen solubility parameters for a carbon fiber/epoxy composite. *Carbon* **2007**, *45*, 2859–2865.
- (29) Dooher, T.; Dixon, D. Multiwalled Carbon Nanotube/Polysulfone Composites: Using the Hildebrand Solubility Parameter to Predict Dispersion. *Polym. Compos.* **2011**, *32*, 1895–1903.
- (30) Usrey, M. L.; Chaffee, A.; Jeng, E. S.; Strano, M. S. Application of Polymer Solubility Theory to Solution Phase Dispersion of Single-Walled Carbon Nanotubes. *J. Phys. Chem. C* **2009**, *113*, 9532–9540.
- (31) Ata, S.; Yamada, T.; Hata, K. Relationship Between Primary Structure and Hansen Solubility Parameter of Carbon Nanotubes. *J. Nanosci. Nanotechnol.* **2017**, *17*, 3310–3315.
- (32) Cardellini, A.; Alberghini, M.; Govind Rajan, A.; Misra, R. P.; Blankschtein, D.; Asinari, P. Multi-scale approach for modeling stability, aggregation, and network formation of nanoparticles suspended in aqueous solutions. *Nanoscale* **2019**, *11*, 3979–3992.
- (33) Lowe, B. M.; Skylaris, C. K.; Green, N. G.; Shibuta, Y.; Sakata, T. Molecular dynamics simulation of potentiometric sensor response: the effect of biomolecules, surface morphology and surface charge. *Nanoscale* **2018**, *10*, 8650–8666.
- (34) Lee, K.; Lim, H. J.; Yang, S. J.; Kim, Y. S.; Park, C. R. Determination of solubility parameters of single-walled and double-walled carbon nanotubes using a finite-length model. *RSC Adv.* **2013**, *3*, 4814–4820.

- (35) Chawla, R.; Sharma, S. Molecular dynamics simulation of carbon nanotube pull-out from polyethylene matrix. *Compos. Sci. Technol.* **2017**, *144*, 169–177.
- (36) Park, C.; Jung, J.; Yun, G. J. Thermomechanical properties of mineralized nitrogen-doped carbon nanotube/polymer nanocomposites by molecular dynamics simulations. *Composites, Part B* **2019**, *161*, 639–650.
- (37) He, Y.; Tang, Y. Thermal conductivity of carbon nanotube/natural rubber composite from molecular dynamics simulations. *J. Theor. Comput. Chem.* **2013**, *12*, 1350011.
- (38) Eslami, H.; Behrouz, M. Molecular Dynamics Simulation of a Polyamide-66/Carbon Nanotube Nanocomposite. *J. Phys. Chem. C* **2014**, *118*, 9841–9851.
- (39) Pramanik, C.; Jamil, T.; Gissinger, J. R.; Guittet, D.; Arias-Monje, P.; Kumar, S.; Heinz, H. Polyacrylonitrile Interactions with Carbon Nanotubes in Solution: Conformations and Binding as a Function of Solvent, Temperature, and Concentration. *Adv. Funct. Mater.* **2019**, *29*, 1905247.
- (40) Gupta, J.; Nunes, C.; Vyas, S.; Jonnalagadda, S. Prediction of solubility parameters and miscibility of pharmaceutical compounds by molecular dynamics simulations. *J. Phys. Chem. B* **2011**, *115*, 2014–23.
- (41) Maiti, A.; Wescott, J.; Kung, P. Nanotube–polymer composites: insights from Flory–Huggins theory and mesoscale simulations. *Mol. Simul.* **2005**, *31*, 143–149.
- (42) Savin, A. V.; Mazo, M. A. The COMPASS force field: Validation for carbon nanoribbons. *Phys. E* **2020**, *118*, 113937.
- (43) Asche, T. S.; Behrens, P.; Schneider, A. M. Validation of the COMPASS force field for complex inorganic-organic hybrid polymers. *J. Sol-Gel Sci. Technol.* **2017**, *81*, 195–204.
- (44) Mayo, S. L.; Olafson, B. D.; Goddard, W. A., III DREIDING: A Generic Force Field for Molecular Simulations. *J. Phys. Chem.* **1990**, *94*, 8897–8909.
- (45) Qiao, B.; Zhao, X.; Yue, D.; Zhang, L.; Wu, S. A combined experiment and molecular dynamics simulation study of hydrogen bonds and free volume in nitrile-butadiene rubber/hindered phenol damping mixtures. *J. Mater. Chem.* **2012**, *22*, 12339–12348.
- (46) Thakral, S.; Thakral, N. K. Prediction of drug-polymer miscibility through the use of solubility parameter based flory-huggins interaction parameter and the experimental validation: PEG as model polymer. *J. Pharm. Sci.* **2013**, *102*, 2254–2263.
- (47) Luo, Y.; Wu, Y.; Luo, K.; Cai, F.; Zhai, T.; Wu, S. Structures and properties of alkanethiol-modified graphene oxide/solution-polymerized styrene butadiene rubber composites: Click chemistry and molecular dynamics simulation. *Compos. Sci. Technol.* **2018**, *161*, 32–38.
- (48) Ma, J.; Larsen, R. M. Effect of Surface Modification on the Hansen Solubility Parameters of Single-Walled Carbon Nanotubes. *Ind. Eng. Chem. Res.* **2013**, *52* (9), 3514–3521.
- (49) Ma, J.; Larsen, R. M. Use of Hansen solubility parameters to predict dispersion and strain transfer of functionalized single-walled carbon nanotubes in poly(vinylidene fluoride) composites. *J. Thermoplast. Compos. Mater.* **2014**, *27*, 801–815.
- (50) Detriche, S.; Nagy, J. B.; Mekhalif, Z.; Delhalle, J. Surface State of Carbon Nanotubes and Hansen Solubility Parameters. *J. Nanosci. Nanotechnol.* **2009**, *9*, 6015–6025.
- (51) Brandao, S. D. F.; Andrada, D.; Mesquita, A. F.; Santos, A. P.; Gorgulho, H. F.; Paniago, R.; Pimenta, M. A.; Fantini, C.; Furtado, C. A. The influence of oxygen-containing functional groups on the dispersion of single-walled carbon nanotubes in amide solvents. *J. Phys.: Condens. Matter* **2010**, *22*, 334222.
- (52) Banhart, F.; Kotakoski, J.; Krasheninnikov, A. V. Structural Defects in Graphene. *ACS Nano* **2011**, *5*, 26–41.
- (53) Luo, Y.; Wang, R.; Wang, W.; Zhang, L.; Wu, S. Molecular Dynamics Simulation Insight Into Two-Component Solubility Parameters of Graphene and Thermodynamic Compatibility of Graphene and Styrene Butadiene Rubber. *J. Phys. Chem. C* **2017**, *121*, 10163–10173.
- (54) Aman-Pommier, F.; Jallut, C. Solubility of diazepam in water plus tert-butyl alcohol solvent mixtures: Part 2. Correlation using Scatchard-Hildebrand and combined Scatchard-Hildebrand/Flory-Huggins excess Gibbs energy models. *Fluid Phase Equilib.* **2018**, *458*, 84–101.